Interface dipole and band bending in the hybrid *p-n* heterojunction MoS_2/GaN(0001)

Hugo Henck,[1] Zeineb Ben Aziza,[1] Olivia Zill,[2] Debora Pierucci,[3] Carl H. Naylor,[4] Mathieu G. Silly,[5] Noelle Gogneau,[1] Fabrice Oehler,[1] Stephane Collin,[1] Julien Brault,[6] Fausto Sirotti,[5] François Bertran,[5] Patrick Le Fèvre,[5] Stéphane Berciaud,[2] A. T. Charlie Johnson,[4] Emmanuel Lhuillier,[7] Julien E. Rault,[5] and Abdelkarim Ouerghi[1,*]

[1]*Centre de Nanosciences et de Nanotechnologies, Centre National de la Recherche Scientifique (CNRS), Univ. Paris-Sud, Université Paris-Saclay, C2N – Marcoussis, 91460 Marcoussis, France*

[2]*Université de Strasbourg, CNRS, Institut de Physique et Chimie des Matériaux de Strasbourg (IPCMS), Unités Mixtes de Recherche (UMR) 7504, F-67000 Strasbourg, France*

[3]*CELLS – ALBA Synchrotron Radiation Facility, Carrer de la Llum 2-26, 08290 Cerdanyola del Vallès, Barcelona, Spain*

[4]*Department of Physics and Astronomy, University of Pennsylvania, 209S 33rd Street, Philadelphia, Pennsylvania 19104, USA*

[5]*Synchrotron SOLEIL, Saint-Aubin, BP48, 91192 Gif sur Yvette Cedex, France*

[6]*Université Côte d'Azur, CNRS, Centre de Recherche sur l'Hétéro-Epitaxie et ses Applications (CRHEA), 06560 Valbonne Sophia Antipolis, France*

[7]*Sorbonne Universités, UPMC Univ. Paris 06, CNRS, UMR 7588, Institut des NanoSciences de Paris, 4 place Jussieu, 75005 Paris, France*

(Received 26 June 2017; published 28 September 2017)

Hybrid heterostructures based on bulk GaN and two-dimensional (2D) materials offer novel paths toward nanoelectronic devices with engineered features. Here, we study the electronic properties of a mixed-dimensional heterostructure composed of intrinsic *n*-doped MoS_2 flakes transferred on *p*-doped GaN(0001) layers. Based on angle-resolved photoemission spectroscopy (ARPES) and high resolution x-ray photoemission spectroscopy (HR-XPS), we investigate the electronic structure modification induced by the interlayer interactions in MoS_2/GaN heterostructure. In particular, a shift of the valence band with respect to the Fermi level for MoS_2/GaN heterostructure is observed, which is the signature of a charge transfer from the 2D monolayer MoS_2 to GaN. The ARPES and HR-XPS revealed an interface dipole associated with local charge transfer from the GaN layer to the MoS_2 monolayer. Valence and conduction band offsets between MoS_2 and GaN are determined to be 0.77 and −0.51 eV, respectively. Based on the measured work functions and band bendings, we establish the formation of an interface dipole between GaN and MoS_2 of 0.2 eV.

DOI: 10.1103/PhysRevB.96.115312

I. INTRODUCTION

Among the vast collection of two-dimensional (2D) materials, transition metal dichalcogenides (TMDs) have attracted considerable interest for their unique layer-dependent electronic and optical properties [1,2]. The TMDs such as MoS_2, $MoSe_2$, WS_2, and WSe_2 have tunable bandgaps from indirect in their bulk form to direct in the monolayer limit, then opening up their wide range of potential applications in nano- (opto-) electronics. For example, MoS_2, one of the most studied TMDs, has been used in field effect transistors [3] with excellent on/off ratio and room temperature mobility and in photodetectors [4] with high responsivity and fast photoresponse. On the other hand, the *p-n* junction is an elementary block of optoelectronics, and its demonstration using 2D TMDs is a mandatory step toward the integration of these materials in real devices [5–10]. Interestingly, the combination of 2D materials grown on a conventional three-dimensional (3D) semiconductor is gaining importance for the design of electronic devices since it combines the advantages of both the established 3D semiconductors and the unique properties of 2D materials. An interesting combination can be obtained using bulk semiconducting GaN and 2D materials [11–16] in the so-called mixed-dimensional heterostructures [17] due to the maturity of planar GaN technology with a broad range of devices spanning from light emitting diodes to high power electronics [18]. Hence, hybridization of GaN with 2D TMDs such as MoS_2 is of particular relevance to design novel hybrid heterostructures. Since theoretical studies on such heterostructures are particularly challenging, experimental research works are mandatory to uncover the 2D TMD/3D heterostructure interfacial and electronic properties and trigger further theoretical efforts. This paper is dedicated to get deeper insight on the electronic properties of the MoS_2/GaN heterostructure as well as the interlayer interaction (i.e., charge transfer) between the two building blocks.

The GaN substrate is suitable for optoelectronic applications. The use of 2D materials and GaN demonstrates examples of a 2D/3D combination matching the general requirements for the vertical heterojunction bipolar transistor. When considering the devices' architecture, the interaction between the 2D layered film and the substrate is crucial. Similarly to 2D van der Waals (vdW) heterostructures [19,20], two key issues have to be considered: the strain effect caused by the lattice mismatch between both materials constituting the heterostructures and the band offsets resulting from the junction formation. Only two works by Tangi *et al.* focused on the interface between GaN/MoS_2 [15] and GaN/WSe_2 [14]. The authors have grown undoped GaN on 2D materials and performed micro-Raman and x-ray photoemission spectroscopy (XPS) to investigate the properties of band alignment in these heterostructures. However, for the optoelectronic applications, an *n*- or a *p*-doped GaN is required. Ruzmetov *et al.* [11] have grown MoS_2 on *n*-type GaN/sapphire. Using conductive atomic

*Corresponding author: mailto:abdelkarim.ouerghi@c2n.upsaclay.fr

force microscopy (CAFM), Ruzmetov *et al.* [11] showed that the MoS_2/GaN heterostructure electrically conduct in the out-of-plane direction and across the vdW gap, forming a promising platform for vertical 2D/3D semiconducting devices. Moreover, Lee *et al.* [13] realized p-MoS_2/n-GaN heterojunction diodes. No Fermi level pinning was present at the interface, and current-voltage measurement of the diodes exhibited excellent rectification. Besides, the influence of the stacking order can modify the electronic properties at the interface. In the meantime, to our knowledge no work in the literature was performed using ARPES to study the electronic structure such as charge transfer, interface dipole, and band bending at n-doped MoS_2 on p-doped GaN interface.

Based on these considerations, the impact of p-doped GaN as a substrate should not be overlooked. The investigation of electronic properties of MoS_2 combined with GaN becomes of fundamental importance. Therefore, based on Raman spectroscopy, we assess the strain sustained by the MoS_2 flakes upon transfer on top of GaN. Next, by using angle resolved photoemission spectroscopy (ARPES), we show a significant charge transfer between the MoS_2 monolayer and the GaN(0001) layer. The ARPES measurements showed that the GaN valence band maximum (VBM) shifts about 300 meV towards the Fermi level compared to the VBM of pristine GaN(0001), implying electron transfer from the GaN layer to MoS_2. Thus, we expect that this experimental study, which offers a better understanding of these heterostructures, will provide sound guidelines towards real industrial applications and will complement the recently introduced 2D/2D approaches [21,22] for which device growth and processing remain quite challenging to scale up.

II. METHODS

The 250-nm-thick p-doped GaN was grown by plasma-assisted molecular beam epitaxy (MBE) on a SiC(0001) substrate. The growth was performed at 730 °C under Ga-rich conditions to favor the 2D growth following the Frank–van der Merwe growth method. During the growth, the Mg cell was kept at 375 °C in order to induce a p-type doping of GaN layer [23]. Large scale MoS_2 monolayer flakes ($\approx$20 to $\approx$ 100 μm) have been grown by chemical vapor deposition (CVD) on oxidized silicon substrate (see Ref. [24]). The MoS_2 flakes transferred onto the GaN retain their triangular shapes with unchanged lateral sizes. Before any measurement, the MoS_2/GaN sample was annealed at 300 °C for 30 min in ultrahigh vacuum ($P \approx 10^{-10}$ mbar) in order to remove the residual surface contaminations induced by the wet transfer. The Raman and photoluminescence (PL) measurements were conducted using a commercial confocal Renishaw micro-Raman microscope with a 532 nm laser in ambient conditions of pressure and temperature. The excitation laser (wavelength 532 nm) was focused onto the samples with a spot diameter of $\sim$1 μm and incident power of $\sim$3 mW. The integration time was optimized in order to obtain an acceptable signal-to-noise ratio. The PL measurements were performed on the same microscope with a 100× objective and a Si detector (detection range up to $\sim$2.2 eV). The XPS experiments were carried out on the TEMPO beamline of Synchrotron SOLEIL at room temperature using a photon energy of 340 eV. The photon source was a HU80 Apple II undulator set to deliver linearly polarized light. The photon energy was selected using a high-resolution (HR) plane grating monochromator, with a resolving power $E/\Delta E$ that can reach 15 000 on the whole energy range (45–1500 eV). During the XPS measurements, the photoelectrons were detected at 0° from the sample surface normal $n^{\rightarrow}$ and at 46° from the polarization vector $E^{\rightarrow}$. The spot size was about 100×80 $(H \times V)$ μm^2. A Shirley background was subtracted in all core level spectra. The Mo 3d spectra were fitted by sums of Voigt curves, i.e., the convolution of a Gaussian (of full-width at half-maximum, GW) by a Lorentzian (of full-width at half-maximum, LW). The LW was fixed at 90 meV. The Ga 3d was fitted with a Voigt curve. The ARPES measurements were conducted at the Cassiopée beamline of Synchrotron SOLEIL. We used horizontal linearly polarized photons of 50 eV and a hemispherical electron analyzer with vertical slits to allow band mapping. The total angle and energy resolutions were 0.25° and 25 meV. The mean diameter of the incident photon beam was smaller than 50 μm. All ARPES experiments were completed at room temperature. The Fermi level reference was taken at the leading edge of a clean metal (i.e., molybdenum clamps) surface in electrical contact with the sample. The cathodoluminescence (CL) measurements were performed with an Attolight Chronos CL microscope operating at room temperature with 2 kV acceleration voltages. An IHR320 spectrometer (Jobin Yvon) connected to a Newton charge-coupled device (CCD) 920 camera (Andor/Oxford Instruments) was used to acquire the CL spectra. The final hypermap is a square matrix of 64×64 pixels, spanning about 30 μm wide, each of them containing a CL spectrum acquired in 1 s. The simulations used to evaluate the CL excitation volume at 2 kV were performed using the CASINO v2.48 software (2D version), using a density of 6.15 g cm^{-3} for the GaN material.

III. RESULTS AND DISCUSSIONS

A 250-nm-thick Mg-doped GaN(0001) (p-doped) grown by plasma-assisted MBE on SiC(0001) was used as a substrate. A few hundred micrometer wide monolayer MoS_2 flakes, grown by CVD on SiO_2 substrate were transferred on the GaN layer by polymethyl methacrylate (PMMA) assisted technique [19] to build a MoS_2/GaN heterostructure, as shown in Fig. 1(a). An annealing process at $T = 300$ °C for 30 min was then used to clean the surface and the interface of our 2D/3D heterostructure. Owing to the large optical absorption of monolayer MoS_2, it is rather simple to identify MoS_2 flakes on the GaN surface, as shown in the optical image in Fig. 1(b). Hence, we can verify that the geometry and the sizes of the MoS_2 flakes are preserved during both transfer and annealing processes.

In Fig. 1(c), we show the micro-Raman spectra in the wavenumber range between 360 and 440 cm^{-1}, obtained for the MoS_2 transferred on GaN (black line) [1]. We can identify the two one-phonon Raman-active modes of monolayer MoS_2, namely the in-plane (E') and out-of-plane (A_1') modes [25,26]. The frequency difference between the frequencies of the A_1' and E' mode features is $\approx$19$-$20 cm^{-1}, a value that is typical from monolayer MoS_2 [see Fig. 1(d)] [19,27]. The Raman intensity maps of the E' and A_1' modes and

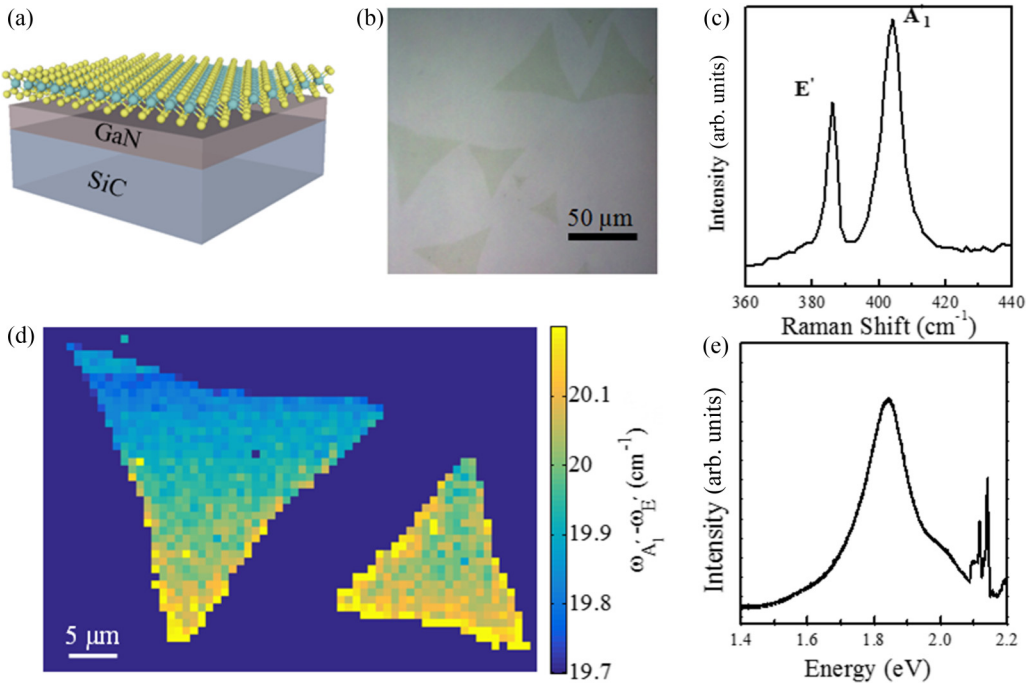

FIG. 1. (a) Schematic of our MoS_2/GaN heterostructure; (b) optical image of MoS_2 transferred on GaN; (c) Raman spectrum of MoS_2/GaN; (d) hyperspectral Raman map of the difference between the frequencies of the A_1' and E' mode features; (e) photoluminescence spectrum of MoS_2/GaN.

the corresponding Raman frequency maps are shown in the Supplemental Material (Fig. S1) [28]. The uniform intensity of both Raman modes illustrates the high quality and the absence of defects in our MoS_2 monolayers. The E' and A_1' mode frequencies display only minute spatial inhomogeneity of $\approx \pm 1\ \mathrm{cm}^{-1}$ over a given MoS_2 single domain [see Fig. 1(d)]. These results indicate that inhomogeneous strain due to the MoS_2 transfer process can be neglected. Figure 1(e) shows the PL spectrum for MoS_2/GaN measured at room temperature. On the PL spectrum, we identify the well-known A and B excitons located near 1.84 and 2 eV, respectively [29]. The A exciton energy is assigned to the optical bandgap of MoS_2 on GaN, which is similar to the value found for vdW heterostructures such as MoS_2/graphene [30].

The XPS and ARPES measurements were carried out for the pristine GaN and MoS_2/GaN(0001) sample not only to investigate the atomic composition and the chemical bonding environment of the interface of our samples but also to uncover the interface-based electronic properties of this heterojunction (band bending, work function, and dipole).

Figure 2(a) shows the XPS spectra of Ga $3d$ for MoS_2/GaN(0001) and the pristine GaN. In the two cases, only one peak is present corresponding to the Ga-N bonds. No oxidation was observed since the Ga $3d$ spectrum did not show any corresponding peak [expected at 1–1.2 eV higher binding energy (BE) with respect to the Ga-N peak [31,32]]. After the MoS_2 transfer on GaN, the Ga $3d$ peak shifts towards lower BE (about 200 meV). This shift at lower BE indicates a variation of the band bending, the result of a charge redistribution at the MoS_2/GaN interface. This effect will be discussed in the next sections.

The Mo $3d$ spectrum [in Fig. 2(b)] contains one main doublet component at BE Mo $3d_{5/2} = 229.7$ eV ($3d_{5/2} : 3d_{3/2}$ ratio of 0.66 and a spin-orbit splitting of 3.10 eV [33]) related to a Mo^{4+} in a sulphur environment [34]. At lower BE (~ -0.52 eV) with respect to the main doublet peaks, a small component is present (highlighted in green), which is the signature of a defective/substoichiometric MoS_2 with sulfur vacancies (Sv) [34,35]. The weight of this component (between 10−15% of the whole Mo $3d$ spectrum) is not representative of a single MoS_2 flake due to the large x-ray spot size [$\sim 100 \times 80\ (H \times V)\ \mu\mathrm{m}^2$], but it gives information on the percentage of defective MoS_2 in the explored area. The shoulder at BE = 226.5 eV represents the sulphur $2s$ peak. These BE values for the Mo $3d$ indicate an intrinsic n-type

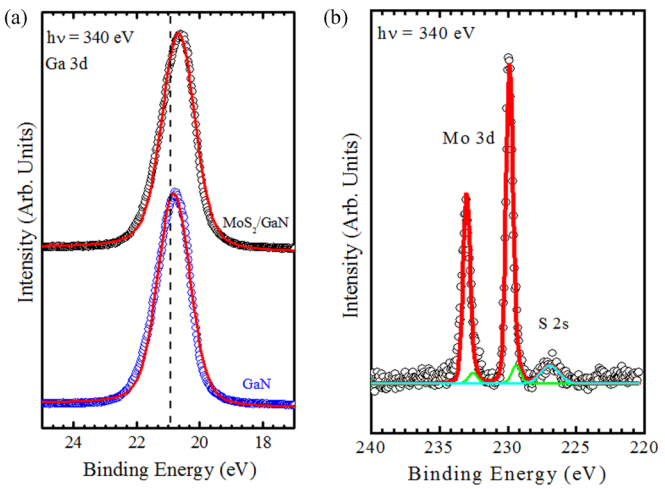

FIG. 2. High-resolution XPS spectra of monolayered MoS_2/GaN heterostructure measured at $h\nu = 340$ eV: (a) Ga-3d for GaN and MoS_2/GaN; (b) Mo-3d for MoS_2/GaN.

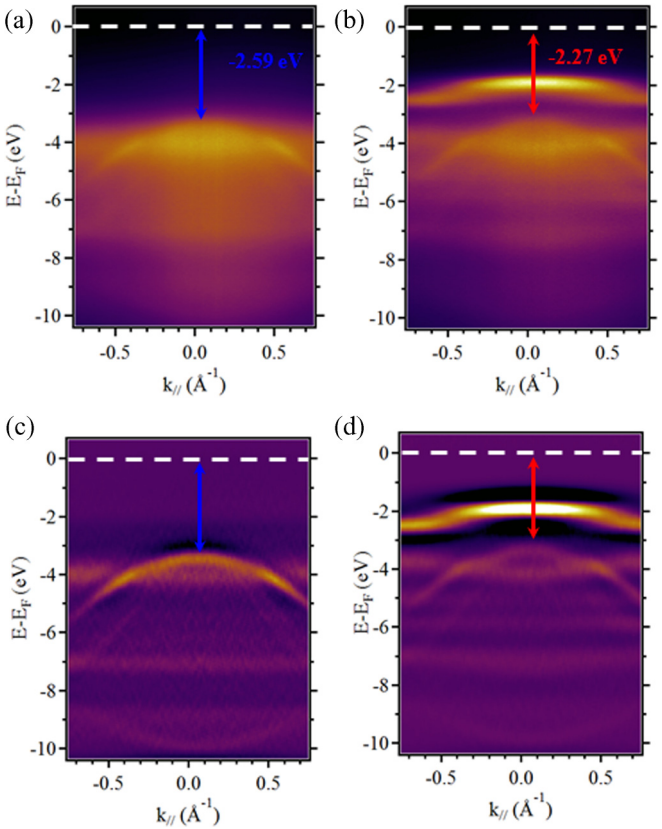

FIG. 3. The ARPES measurements of (a) GaN and (b) MoS_2/GaN measured at $h\nu = 50$ eV around the Γ point of Brillouin zones; the inserts in (a) and (b) correspond to the Brillouin zones of GaN and MoS_2/GaN, respectively. (c) and (d) The second-derivative spectra of (a) and (b), respectively, giving better visibility of the bands.

doping of the MoS_2 flakes [36]. No other components are present on the Mo 3*d* spectrum related to nitrogen, oxygen, or carbon bonds [37–39], indicating that no contaminations are present on the sample and confirming the high quality of the interface of this hybrid heterostructure. Moreover, there is no signature of any chemical state associated with Mo or S in the Ga 3*d* core level spectrum, which is clear evidence of a vdW interaction between MoS_2 and GaN. This makes the heterointerface atomically abrupt without any interdiffusion.

In order to investigate the band alignment and the electronic properties of the hybrid MoS_2/GaN heterostructure, we performed band structure measurements by ARPES at the Cassiopée beamline of Synchrotron SOLEIL. The photoelectron intensity as a function of energy and *k* momentum of pristine GaN(0001) and hybrid MoS_2/GaN(0001) are presented in Figs. 3(a) and 3(b), respectively. The respective second-derivative spectra are provided in Figs. 3(c) and 3(d) to improve the visibility of the band structure. The valence band structure of GaN is shown in Figs. 3(a) and 3(c). From Figs. 3(b) and 3(d), we notice the appearance of a new top-most band at around −1.5 eV, which is the signature of MoS_2 valence band. This confirms the high quality of the transferred MoS_2 within the hybrid heterostructure. We also can notice that the topmost band of GaN is upshifted upon the MoS_2 transfer.

In Fig. 4(a) is shown a vertical section at $k_{\parallel} = 0\,\text{Å}^{-1}$ of the band structure of the MoS_2/GaN heterostructure and the pristine GaN. From the intersection of the linear extrapolation of the leading edge of the valence band spectrum with the baseline, we can locate the position of the VBM for the GaN in the heterostructure with respect to the pristine one. The relative VBM positions moved from 2.59 to 2.27 ± 0.05 eV for the GaN(0001) layer and the MoS_2/GaN heterostructure, respectively. This value is in agreement with the observed band shift in ARPES measurements. This implies that VBM is getting closer to the Fermi level (located at 0 eV), reducing the band bending (V_{BB}) at the interface of about $\Delta V_{BB} = 0.32$ eV. The valence band for the pristine GaN was also measured with a photon energy $h\nu = 1300$ eV (see Fig. S2 in the Supplemental Material [28]). Using this photon energy, a probing depth of about 10 nm is reached, which is reasonably larger than the depletion region at the GaN interface. Then using the same procedure used in Fig. 4, the distance of the valence band to the Fermi level $E_v = 0.70 \pm 0.05$ eV in the bulk (i.e., in a flat band condition) was obtained. Considering that at the surface the VBM = 2.27 eV, a downward band bending of about 1.57 eV is present at the GaN(0001) surface. This band bending corresponds to an accumulation of positive charge at the GaN surface, compensated by an opposite negative charge inside the semiconductor (i.e., depletion layer). When the MoS_2/GaN heterostructure is formed, this band bending is reduced. This effect is the result of electron transfer (interface dipole formation) from GaN(0001) in favor of MoS_2. From Fig. 4(a), we are also able to infer more precisely the VBM for the MoS_2, VBM $= 1.50 \pm 0.05$ eV, which implies a valence band offset between MoS_2 and GaN (ΔE_v) of about 0.77 eV. To gain insight into the electronic properties of the MoS_2/GaN interface, the work function of the heterostructure was compared to the work function of the pristine GaN via the measurement of the secondary electron cutoff [Fig. 4(b)]. We found a work function of $\phi = 5.23 \pm 0.05$ eV for pristine GaN and $\phi = 5.35 \pm 0.05$ eV for the hybrid MoS_2/GaN heterostructure. Based on literature about probing quasiparticle band structure by scanning tunneling microscopy/scanning tunneling spectroscopy STM/STS [22], the bandgap of MoS_2 is about 2.15 eV. This MoS_2 electronic bandgap is larger than its optical bandgap, determined previously by PL spectroscopy [∼1.84 eV; see Fig. 1(e)] considering the large exciton BE in atomically thin TMDs [40]. The CL experiments described in Fig. S3 (see the Supplemental Material [28]) were performed to further probe the MoS_2/GaN interface. From Fig. 4(c), we determine a value of 3.41 ± 0.01 eV for the GaN optical gap at room temperature, consistent with the reported value of wurtzite GaN [41]. Considering the exciton BE in GaN of about 0.02 eV [31], we deduce a GaN excitonic gap of about $3.43\,\text{eV} \pm 0.01$ eV. Thus, with the known values of the bandgaps (MoS_2 and GaN), the conduction band discontinuity ΔE_C is calculated from $\Delta E_C = \Delta E_V - (E_{MoS2} - E_{GaN})$, where E_{MoS2} and E_{GaN} are the bandgap energies of MoS_2 and GaN, respectively; we obtain $\Delta E_C = -0.51$ eV with type II band alignment at *n*-MoS_2/*p*-GaN heterojunction. This conduction band offset is close to the recently reported value (0.56 eV) for intrinsic epitaxial GaN/MoS_2 [15], with an inverted band position with respect to our work (i.e., the GaN CBM is at

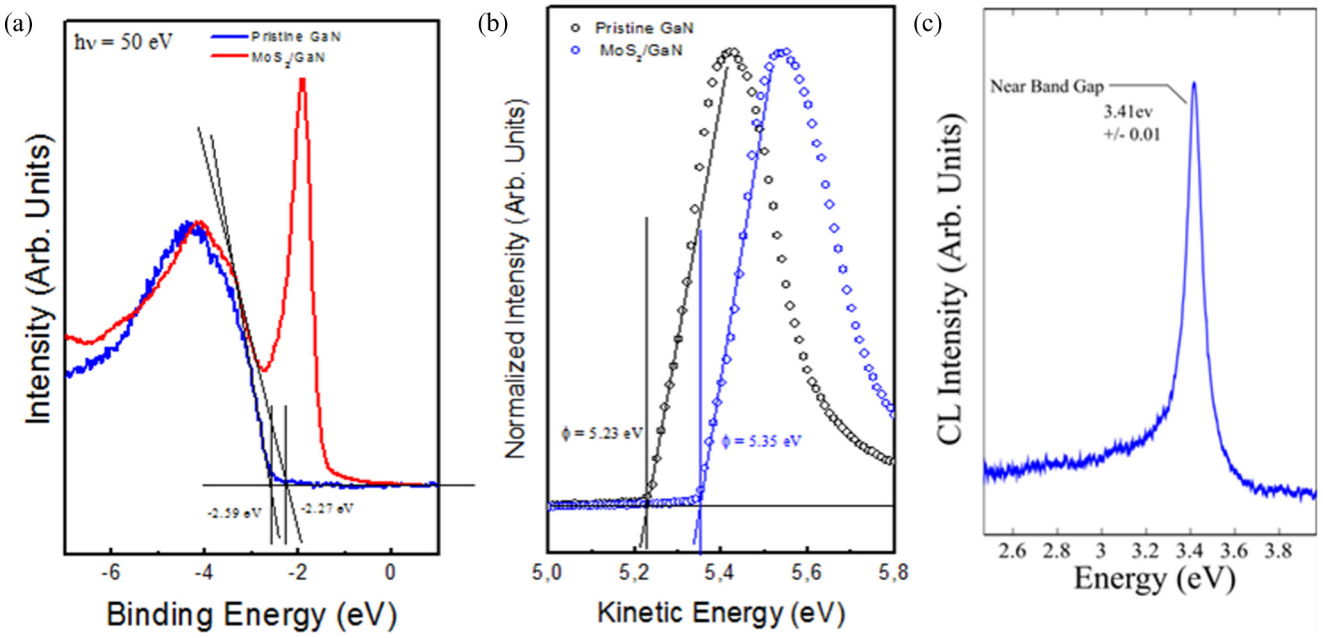

FIG. 4. (a) Integrated valence band at at $k_{\parallel} = 0\,\text{Å}^{-1}$ of MoS_2/GaN and GaN at $h\nu = 50\,\text{eV}$; (b) secondary electron cutoff vs kinetic energy of pristine GaN and MoS_2/GaN; (c) CL of GaN.

higher BE with respect to the MoS_2 CBM). A different band alignment was obtained in the case of n-doped GaN/p-doped MoS_2 [13], where a conduction band offset of 0.23 eV was measured. These results suggest the possibility of tuning the relative band alignment in the 2D/3D heterostructure and then the potential barrier height at the junction by varying the doping of the MoS_2 and the GaN layers. Although electronic properties in 2D materials are generally governed by interactions at the K points of the Brillouin zones due to direct bandgap around this particular point, the presence of a direct bandgap centered at the Γ point in the GaN electronic structure suggests that charge transfer is not trivial in this heterostructure. By combining all the photoemission studies, an interface electronic structure diagram is derived (Fig. 5). These findings are in agreement with what was observed for WS_2/p-doped GaN [42], where an efficient charge transfer at the 2D-3D heterointerface was observed. In particular, Kummel *et al.* [42] have shown that for this 2D/3D heterostructure, the efficiency of the charge transfer across the heterointerface is influenced by the momentum mismatch of the VBM in the two semiconductors. Specifically, they underlined that the charge transfer process is more efficient when the excitation in the k space is near the Γ point of the 2D semiconductor, where a transfer to the 3D substrate is possible without a momentum change. At variance with metal, the work function of a semiconductor is not an intrinsic property simply because the position of the Fermi level in the gap at the surface depends on the doping of the substrate, which determines the amount of band bending. Moreover, when we form the MoS_2/GaN heterostructure, a surface dipole ($\Delta\phi_{\text{Dip}}$) could be formed at the interface. This effect is described by the measured variation of work function of the system ($\Delta\phi = 0.12\,\text{eV}$). We have to take into account that in the case of a semiconductor, the variation of band bending at the surface ($\Delta V_{\text{BB}} = 0.32\,\text{eV}$) also contributes to the total work function change. The effect of dipole $\Delta\phi_{\text{Dip}}$ is assumed to change the electron affinity χ (where the electron affinity is the energy difference between the vacuum level E_{VAC} and the conduction

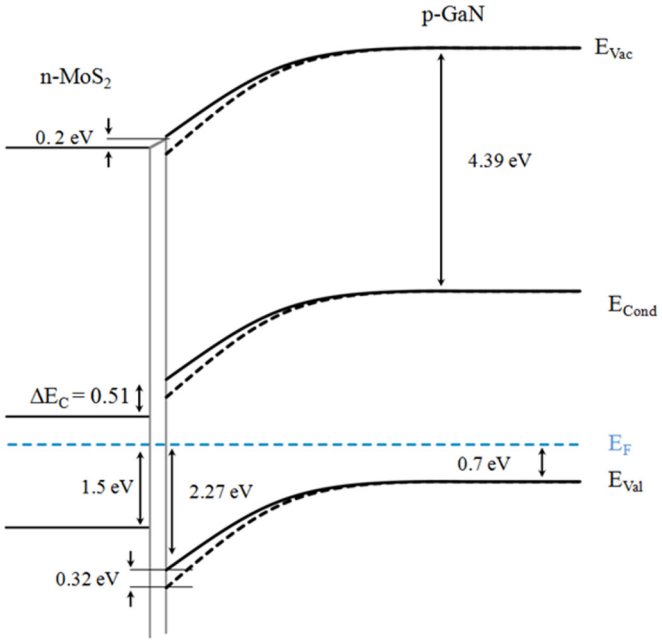

FIG. 5. Schematic of band alignment diagram of MoS_2/GaN heterostructure obtained from XPS/ARPES and CL measurements. The bandgap values of MoS_2 and GaN have been obtained considering their excitons binding energies [30,39]. The solid and dashed lines correspond, respectively, to the band bending after and before MoS_2 transfer highlighting a variation of the band bending in GaN after MoS_2 transfer.

band at the surface E_{CBM}). Thus the total work function change $\Delta\phi$ due to the heterostructure formation is

$$\Delta\phi = \Delta\chi + \Delta V_{BB} = \Delta\phi_{Dip} + \Delta V_{BB}.$$

From this formula and the measured $\Delta\phi$ and ΔV_{BB}, we calculate a surface dipole of $\Delta\phi_{Dip} = 0.2\,eV$. This interface dipole is a consequence of interface electron redistribution between the single layer of MoS_2 and GaN(0001). This does not imply any chemical bonding between the GaN and the MoS_2. Such charge redistribution at the interface between GaN and MoS_2 is also in agreement with GaSe/graphene [8,43] and graphene/MoS_2 [30] heterostructures previously reported. It is interesting to underline also that the Ga 3*d* core level peak shifts by a lesser amount compared to the VBM after the heterostructure formation; this is probably related to this difference in the interface properties, e.g., this dipole formation.

IV. CONCLUSIONS

In summary, the interaction of *n*-doped single layer MoS_2 on top of *p*-doped GaN layer was systematically studied via various characterization methods. An interfacial charge transfer was highlighted within the hybrid heterostructure using ARPES. Based on our measurements, we propose a band diagram model to explain the charge doping effect deducing a conduction band discontinuity of about $\Delta E_C = 0.51\,eV$ in a type II alignment configuration. The experimental band alignment is determined by XPS/ARPES measurements comparing the effect of MoS_2 transfer on the electronic structure of GaN. Therefore, the heterointerface formation gives rise to an additional dipole change of 0.2 eV, which could shift the band edges with respect to each other. The band alignment obtained in the present paper represents an essential information for building electronic and optoelectronic devices based on the GaN/monolayer MoS_2 and, to a larger extent, for understanding the electronic coupling in 2D/3D heterostructures.

ACKNOWLEDGMENTS

We acknowledge support from the Agence Nationale de la Recherche (ANR) under grants Labex GANEX (Grant No. ANR-11-LABX-0014), Labex Nanosaclay (Grant No. ANR-10-LABX-0035), and H2DH (Grant No. ANR-15-CE24-0016), from the Region Ile-de-France in the framework of C'Nano IdF (nanoscience competence center of Paris Region), and from the European Union (FEDER 2007-2013). Labex GANEX and Nanosaclay belongs to the public funded Investissements d'Avenir program managed by ANR. S.B. is a member of Institut Universitaire de France (IUF). C.H.N. and A.T.C.J. Acknowledge support from the National Science Foundation EFRI-2DARE program, Grant No. ENG- 1542879.

[1] G. R. Bhimanapati, Z. Lin, V. Meunier, Y. Jung, J. Cha, S. Das, D. Xiao, Y. Son, M. S. Strano, V. R. Cooper, L. Liang, S. G. Louie, E. Ringe, W. Zhou, S. S. Kim, R. R. Naik, B. G. Sumpter, H. Terrones, F. Xia, Y. Wang, J. Zhu, D. Akinwande, N. Alem, J. A. Schuller, R. E. Schaak, M. Terrones, and J. A. Robinson, Recent advances in two-dimensional materials beyond graphene, ACS Nano **9**, 11509 (2015).

[2] Q. H. Wang, K. Kalantar-Zadeh, A. Kis, J. N. Coleman, and M. S. Strano, Electronics and optoelectronics of two-dimensional transition metal dichalcogenides, Nat. Nanotechnol. **7**, 699 (2012).

[3] B. Radisavljevic, A. Radenovic, J. Brivio, V. Giacometti, and A. Kis, Single-layer MoS_2 transistors, Nat. Nanotechnol. **6**, 147 (2011).

[4] F. H. Koppens, T. Mueller, P. Avouris, A. C. Ferrari, M. S. Vitiello, and M. Polini, Photodetectors based on graphene, other two-dimensional materials and hybrid systems, Nat. Nanotechnol. **9**, 780 (2014).

[5] X. Li, M.-W. Lin, J. Lin, B. Huang, A. A. Puretzky, C. Ma, K. Wang, W. Zhou, S. T. Pantelides, M. Chi, I. Kravchenko, J. Fowlkes, C. M. Rouleau, D. B. Geohegan, and K. Xiao, Two-dimensional GaSe/$MoSe_2$ misfit bilayer heterojunctions by van der Waals epitaxy, Sci. Adv. **2**, e1501882 (2016).

[6] F. Wang, Z. Wang, K. Xu, F. Wang, Q. Wang, Y. Huang, L. Yin, and J. He, Tunable GaTe-MoS_2 van der Waals p-n junctions with novel optoelectronic performance, Nano Lett. **15**, 7558 (2015).

[7] C.-H. Lee, G.-H. Lee, A. M. van der Zande, W. Chen, Y. Li, M. Han, X. Cui, G. Arefe, C. Nuckolls, T. F. Heinz, J. Guo, J. Hone, and P. Kim, Atomically thin p-n junctions with van der Waals heterointerfaces, Nat. Nanotechnol. **9**, 676 (2014).

[8] Z. Ben Aziza, H. Henck, D. Pierucci, M. G. Silly, E. Lhuillier, G. Patriarche, F. Sirotti, M. Eddrief, and A. Ouerghi, van der Waals epitaxy of GaSe/graphene heterostructure: Electronic and interfacial properties, ACS Nano **10**, 9679 (2016).

[9] H. Henck, D. Pierucci, J. Chaste, C. H. Naylor, J. Avila, A. Balan, M. G. Silly, C. Maria, F. Sirotti, A. T. C. Johnson, E. Lhuillier, A. Ouerghi, H. Henck, D. Pierucci, J. Chaste, C. H. Naylor, J. Avila, A. Balan, M. G. Silly, M. C. Asensio, F. Sirotti, A. T. C. Johnson, E. Lhuillier, and A. Ouerghi, Electrolytic phototransistor based on graphene-MoS_2van der Waals p-n heterojunction with tunable photoresponse p-n heterojunction with tunable photoresponse, Appl. Phys. Lett. **109**, 113103 (2016).

[10] D. Sarkar, X. Xie, W. Liu, W. Cao, J. Kang, Y. Gong, S. Kraemer, P. M. Ajayan, and K. Banerjee, A subthermionic tunnel field-effect transistor with an atomically thin channel, Nature **526**, 91 (2015).

[11] D. Ruzmetov, K. Zhang, G. Stan, B. Kalanyan, G. R. Bhimanapati, S. M. Eichfeld, R. A. Burke, P. B. Shah, T. P. O'Regan, F. J. Crowne, A. G. Birdwell, J. A. Robinson, A. V. Davydov, and T. G. Ivanov, Vertical 2D/3D semiconductor heterostructures based on epitaxial molybdenum disulfide and gallium nitride, ACS Nano **10**, 3580 (2016).

[12] C. H. Lee, S. Krishnamoorthy, D. J. O'Hara, J. M. Johnson, J. Jamison, R. C. Myers, R. K. Kawakami, J. Hwang, and S. Rajan, Molecular beam epitaxy of 2D-layered gallium selenide on GaN substrates, J. Appl. Phys. **121**, 094302 (2017).

[13] E. W. Lee, C. H. Lee, P. K. Paul, L. Ma, W. D. McCulloch, S. Krishnamoorthy, Y. Wu, A. R. Arehart, and S. Rajan, Layer-Transferred MoS_2/GaN PN Diodes, Appl. Phys. Lett. **107**, 103505 (2015).

[14] M. Tangi, P. Mishra, C.-C. Tseng, T. K. Ng, M. N. Hedhili, D. H. Anjum, M. S. Alias, N. Wei, L.-J. Li, and B. S. Ooi,

Band alignment at GaN/single-layer WSe_2 interface, ACS Appl. Mater. Interfaces **9**, 9110 (2017).

[15] M. Tangi, P. Mishra, T. K. Ng, M. N. Hedhili, B. Janjua, M. S. Alias, D. H. Anjum, C. C. Tseng, Y. Shi, H. J. Joyce, L. J. Li, and B. S. Ooi, Determination of band offsets at GaN/single-layer MoS_2 heterojunction, Appl. Phys. Lett. **109**, 032104 (2016).

[16] T. P. O'Regan, D. Ruzmetov, M. R. Neupane, R. A. Burke, A. A. Herzing, K. Zhang, A. G. Birdwell, D. E. Taylor, E. F. C. Byrd, S. D. Walck, A. V. Davydov, J. A. Robinson, and T. G. Ivanov, Structural and electrical analysis of epitaxial 2D/3D vertical heterojunctions of monolayer MoS_2 on GaN, Appl. Phys. Lett. **111**, 051602 (2017).

[17] D. Jariwala, T. J. Marks, and M. C. Hersam, Mixed-dimensional van der Waals heterostructures, Nat. Mater. **16**, 170 (2016).

[18] M. S. Kang, C. H. Lee, J. B. Park, H. Yoo, and G. C. Yi, Gallium nitride nanostructures for light-emitting diode applications, Nano Energy **1**, 391 (2012).

[19] D. Pierucci, H. Henck, C. H. Naylor, H. Sediri, E. Lhuillier, A. Balan, J. E. Rault, Y. J. Dappe, F. Bertran, P. Le Févre, A. T. C. Johnson, and A. Ouerghi, Large area molybdenum disulphide-epitaxial graphene vertical van der Waals heterostructures, Sci. Rep. **6**, 26656 (2016).

[20] X. Hong, J. Kim, S.-F. Shi, Y. Zhang, C. Jin, Y. Sun, S. Tongay, J. Wu, Y. Zhang, and F. Wang, Ultrafast charge transfer in atomically thin MoS_2/WS_2 heterostructures, Nat. Nanotechnol. **9**, 682 (2014).

[21] T. Georgiou, R. Jalil, B. D. Belle, L. Britnell, R. V. Gorbachev, S. V. Morozov, Y.-J. Kim, A. Gholinia, S. J. Haigh, O. Makarovsky, L. Eaves, L. A. Ponomarenko, A. K. Geim, K. S. Novoselov, and A. Mishchenko, Vertical field effect transistor based on graphene-WS_2 heterostructures for flexible and transparent electronics, Nat. Nanotechnol. **8**, 100 (2012).

[22] M.-H. Chiu, C. Zhang, H.-W. Shiu, C.-P. Chuu, C.-H. Chen, C.-Y. S. Chang, C.-H. Chen, M.-Y. Chou, C.-K. Shih, and L.-J. Li, Determination of band alignment in the single-layer MoS_2/WSe_2 heterojunction, Nat. Commun. **6**, 7666 (2015).

[23] R. R. Lieten, V. Motsnyi, L. Zhang, K. Cheng, M. Leys, S. Degroote, G. Buchowicz, O. Dubon, and G. Borghs, Mg doping of GaN by molecular beam epitaxy, J. Phys. D. Appl. Phys. **44**, 135406 (2011).

[24] G. H. Han, N. J. Kybert, C. H. Naylor, B. S. Lee, J. Ping, J. H. Park, J. Kang, S. Y. Lee, Y. H. Lee, R. Agarwal, and A. T. C. Johnson, Seeded growth of highly crystalline molybdenum disulphide monolayers at controlled locations, Nat. Commun. **6**, 6128 (2015).

[25] Y. Wang, C. Cong, C. Qiu, and T. Yu, Raman spectroscopy study of lattice vibration and crystallographic orientation of monolayer MoS_2 under uniaxial strain, Small **9**, 2857 (2013).

[26] C. Lee, H. Yan, L. E. Brus, T. F. Heinz, J. Hone, and S. Ryu, Anomalous lattice vibrations of single- and few-layer MoS_2, ACS Nano **4**, 2695 (2010).

[27] Z. Ben Aziza, H. Henck, D. Di Feliceb, D. Pierucci, J. Chaste, C. H. Naylor, A. Balan, Y. J. Dappe, A. T. C. Johnson, and A. Ouerghi, Bandgap inhomogeneity of MoS_2 monolayer on epitaxial graphene bilayer in van der Waals p-n junction, Carbon N. Y. **110**, 396 (2016).

[28] See Supplemental Material at http://link.aps.org/supplemental/10.1103/PhysRevB.96.115312 for Raman spectroscopie, XPS measurements and cathodoluminescence experiments.

[29] G. Eda, H. Yamaguchi, D. Voiry, T. Fujita, M. Chen, and M. Chhowalla, Photoluminescence from chemically exfoliated MoS_2, Nano Lett. **11**, 5111 (2011).

[30] D. Pierucci, H. Henck, J. Avila, A. Balan, C. H. Naylor, G. Patriarche, Y. J. Dappe, M. G. Silly, F. Sirotti, A. T. C. Johnson, M. C. Asensio, and A. Ouerghi, Band alignment and minigaps in monolayer MoS_2-graphene van der Waals heterostructures, Nano Lett. **16**, 4054 (2016).

[31] S. S. Kushvaha, M. S. Kumar, A. K. Shukla, B. S. Yadav, D. K. Singh, M. Jewariya, S. R. Ragam, and K. K. Maurya, Structural, optical and electronic properties of homoepitaxial GaN nanowalls grown on GaN template by laser molecular beam epitaxy, RSC Adv. **5**, 87818 (2015).

[32] M. Mishra, T. C. S. Krishna, N. Aggarwal, and G. Gupta, Surface chemistry and electronic structure of nonpolar and polar GaN films, Appl. Surf. Sci. **345**, 440 (2015).

[33] S. Mattila, J. A. Leiro, M. Heinonen, and T. Laiho, Core level spectroscopy of MoS_2, Surf. Sci. **600**, 5168 (2006).

[34] I. S. Kim, V. K. Sangwan, D. Jariwala, J. D. Wood, S. Park, K. S. Chen, F. Shi, F. Ruiz-Zepeda, A. Ponce, M. Jose-Yacaman, V. P. Dravid, T. J. Marks, M. C. Hersam, and L. J. Lauhon, Influence of stoichiometry on the optical and electrical properties of chemical vapor deposition derived MoS_2, ACS Nano **8**, 10551 (2014).

[35] W. Zhou, X. Zou, S. Najmaei, Z. Liu, Y. Shi, J. Kong, J. Lou, P. M. Ajayan, B. I. Yakobson, and J.-C. Idrobo, Intrinsic structural defects in monolayer molybdenum disulfide, Nano Lett. **13**, 2615 (2013).

[36] R. Addou, S. Mcdonnell, D. Barrera, Z. Guo, A. Azcatl, J. Wang, H. Zhu, C. L. Hinkle, M. Quevedo-lopez, H. N. Alshareef, L. Colombo, J. W. P. Hsu, and R. M. Wallace, Impurities and electronic property variations of natural MoS_2 crystal surfaces, ACS Nano **9**, 9124 (2015).

[37] A. Levasseur, P. Vinatier, and D. Gonbeau, X-ray photoelectron spectroscopy: A powerful tool for a better characterization of thin film materials, Bull. Mater. Sci. **22**, 607 (1999).

[38] M. A. Baker, R. Gilmore, C. Lenardi, and W. Gissler, XPS investigation of preferential sputtering of S from MoS_2 and determination of MoS_X stoichiometry from Mo and S peak positions, Appl. Surf. Sci. **150**, 255 (1999).

[39] P. D. Fleischauer and J. R. Lince, A comparison of oxidation and oxygen substitution in MoS_2 solid film lubricants, Tribol. Int. **32**, 627 (1999).

[40] M. M. Ugeda, A. J. Bradley, S.-F. Shi, F. H. da Jornada, Y. Zhang, D. Y. Qiu, W. Ruan, S.-K. Mo, Z. Hussain, Z.-X. Shen, F. Wang, S. G. Louie, and M. F. Crommie, Giant bandgap renormalization and excitonic effects in a monolayer transition metal dichalcogenide semiconductor, Nat. Mater. **13**, 1091 (2014).

[41] S. Strite and H. Morkoç, GaN, AlN, and InN: A review, J. Vac. Sci. Technol. B Microelectron. Nanom. Struct. Process. Meas. Phenom. **10**, 1237 (1992).

[42] T. Kummell, U. Hutten, F. Heyer, K. Derr, R. M. Neubieser, W. Quitsch, and G. Bacher, Carrier transfer across a 2D-3D semiconductor heterointerface: The role of momentum mismatch, Phys. Rev. B **95**, 081304 (2017).

[43] C. Si, Z. Lin, J. Zhou, and Z. Sun, Controllable Schottky barrier in GaSe/graphene heterostructure: The role of interface dipole, 2D Mater. **4**, 015027 (2016).